Copper-based reversible electrochemical mirror device with switchability between transparent, blue, and mirror states

Eh, Alice Lee-Sie; Lin, Meng-Fang; Cui, Mengqi; Cai, Guofa; Lee, Pooi See

2017

Eh, A. L.-S., Lin, M.-F., Cui, M., Cai, G., & Lee, P. S. (2017). Copper-based reversible electrochemical mirror device with switchability between transparent, blue, and mirror states. Journal of Materials Chemistry C, 5(26), 6547-6554.

https://hdl.handle.net/10356/83304

https://doi.org/10.1039/C7TC01070B

View Article Online
DOI: 10.1039/C7TC01070B

Journal of
Materials Chemistry C

PAPER

Copper-based reversible electrochemical mirror device with switchability between transparent, blue, and mirror states

Received 00th January 20xx,
Accepted 00th January 20xx

DOI: 10.1039/x0xx00000x

www.rsc.org/MaterialsC

Alice Lee-Sie Eh, Meng-Fang Lin, Mengqi Cui, Guofa Cai, and Pooi See Lee*

Reversible electrochemical mirror (REM) device can be electrochemically tuned to exhibit dual transmittance and reflectance modulations in a single device. Conventional REM devices reversibly switched between transparent and mirror states. However, it is of great challenge to maintain the mirror state of the REM devices due to the diffusion of anions into the metallic film at the open-circuit state. In this work, we report a Cu-based REM device which offers reversible switching between transparent, blue and mirror states with judicious selection of electrolyte and controllable electrodeposition. The blue state can be obtained through the formation of copper (I) chloride, CuCl, when copper (II) chloride $CuCl_2$ undergoes electrochemical reduction. The polymer host, PVA (poly(vinyl alcohol)) plays an important role in reducing the surface roughness of the electrodeposited mirror film, improving film uniformity and sustaining the mirror state of the device during the voltage-off state.

1. Introduction

Sustainable energy has been making headlines in recent years, citing depleting fossil fuel reserves and climate change as the unresolved challenges. Emerging technologies provide viable solutions to exploit renewable energy resources and conserve energy consumption to promote sustainability. Fenestration technology in buildings such as electrochromic has benchmarked itself among various smart windows technologies in the race towards providing the end-users with energy efficient solutions. Electrochromism is defined as the ability of a material to change its optical properties such as transmittance, reflectance and absorption within specific range of the electromagnetic spectrum under an applied voltage[1-7]. Electrochromics are attractive from the application point of view, particularly in solar control in architectural buildings[8-12], flat panel displays[13,14] and spacecraft thermal control[15,16] as they can reversibly modulate optical properties upon the application of electrical bias. The basic requirement for a functional electrochromic material is the electrochemical redox behavior with the ability to modulate the optical properties upon electrical bias.

Electrochromic materials can be categorized into three different groups. The first category consisted of transition metal oxides (TMOs) such as tungsten oxide (WO_3,) vanadium pentoxide (V_2O_5), nickel oxide (NiO) and polymers like polyaniline and poly(3,4-ethylenedioxythiophene)-poly(styrenesulfonate)[4,6,17,18]. Color switching takes place on charge/discharge by simultaneous ions (H^+, Li^+, Na^+) and electrons injection/extraction with an application of electrical potential[19-21]. The second category involves hydrogen-induced phase transitions in rare earths, and mixtures of transition metals/rare earth with magnesium, to achieve variable reflectivity[22,23]. This switchable mirror glass changes its optical properties between two different states (transparent and reflective) via hydrogenation and dehydrogenation of the films[22,24-27]. The third category involves reversible electrodeposition and dissolution of materials such as metals (Ag, Bi, Al, Pb, Cu, Ni) and viologens onto a transparent conductor, hence affecting its optical properties[28-44]. For the first two categories, the electrochromic materials are coated onto the transparent conductors prior to device assembly. Typically, solid state coatings can be prepared via sputtering[45], ultra-high vacuum evaporation[46], pulsed electrodeposition[4], spray-coating[18], spin-coating[9], inkjet-printing[6,47], ultrasonic spray pyrolysis[48], and layer-by-layer assembly[49]. Those techniques are not cost-effective and time consuming. On the contrary, REM devices do not require tedious pre-coating. Instead, the reversible electrodeposition materials are dissolved in the electrolyte and formed thin film on the conducting substrate with the passage of electric current; film dissolution takes place upon reverse bias, producing the optical modulation[28].

Reversible electrochemical mirrors (REMs) are designed to modulate their reflectance from a highly reflective state, enough to mirror a subject, to a highly transparent state in response to external stimuli such as electricity[36-38, 50,51]. These tunable mirrors hold the technological promises for applications such as information displays, optic devices and smart windows[36, 37, 47, 52-54]. Nevertheless, this technology has yet to reach widespread practical applications due to critical issues such as poor uniformity of electrodeposited film, poor stability of the mirror state, and slow switching time[37,55]. To enhance the uniformity of the electrodeposited mirror film, thin nucleation or surface modification layer is often

*School of Materials Science and Engineering, Nanyang Technological University, 50 Nanyang Avenue, Singapore 639798, Singapore. *Email: pslee@ntu.edu.sg; Web: http://www.ntu.edu.sg/home/pslee/*

Electronic Supplementary Information (ESI) available: See DOI: 10.1039/x0xx00000x

View Article Online
DOI: 10.1039/C7TC01070B

introduced to improve the nucleation sites. Typically, a noble metal such as platinum, gold, palladium, and rhodium is used for the promotion of nucleation sites for the metal electrodeposition to attain a continuous and fine-grained metal film with high reflectivity[55]. Maintaining the mirror state of the REM device is rather challenging due to the anions are prone to diffuse into the metallic film at the open-circuit state[37]. Often, continuous application of reduction voltage is required to avoid the dissolution of metallic film into the electrolyte. However, prolonged electrical bias will yield cracks and wrinkles on the metal films due to the poor adhesion and aggregation of metal nanoparticles on the transparent conducting electrode[37]. The susceptibility to dendrite formation at or near mirror electrode can adversely affect the electrochemical performance of the device, and in severe circumstances may render the device inoperable[56]. Therefore, Park *et. al.* introduced ionic liquid as an anion-blocking layer in the electrolyte formulation to achieve long memory effect which effectively formed a barrier against the bromide ions and protected the Ag metal thin film in the voltage-off state[37], allowing longer memory effect. The possible drawback of using ionic liquid-based electrolytes is that ionic liquids are fairly expensive and highly sensitive to moisture[57,58]. For display applications, the key drawback of reversible metal electrodeposition is the relatively slow response in attaining adequate light blockage[55, 59]. The most intriguing feature of the REM devices is the capability to offer dual absorption and reflection in a single device. Araki *et. al.* has developed Ag-based device that can exhibit three optical states (transparent, black and mirror) by modification of the ITO electrode[36].

In this work, we developed a facile electrolyte preparation using copper chloride ($CuCl_2$) that can be reversibly electrodeposited and dissolved back into dimethyl sulfoxide (DMSO)-based electrolyte. Compared to the conventional Ag material for the REM device, Cu has a ubiquitous source, stable market price, high thermal and electrical conductivity and recyclability, rendering its massive applicability in sustainable electronics. In view of its high reflectivity and electroactivity, Cu-based REM device could find numerous applications in reflective displays, energy saving smart windows for buildings and automobiles. Current state of the art trivializes Cu as the electrochemical mediator rather than appreciating it as the reversible electrodeposition material[36-38]. For instance, copper is a prerequisite electrochemical mediator in initiating Ag film dissolution in the Ag-based REM device as it promotes reversibility[36]. With the addition of a polymer host, PVA in the electrolyte, we hypothesized that memory effect can be sustained with the retarded diffusion of anions through the viscous polymeric gel electrolyte into the Cu film and thus hinders the film from fast dissolution. The blue state can be obtained through the formation of CuCl, when $CuCl_2$ undergoes electrochemical reduction. Herein, we present a Cu-based REM device which offers transmittance and reflectance modulations with three reversible switchable states of transparent, blue and mirror states. This is the first time a new color state is introduced in the REM device via different route. Conventional REM device is often limited to switchability between the transparent and mirror states[37,38]. Recent works introduced the black color state in the REM device through modification of the ITO or FTO electrodes[36,51]. We demonstrated that by carefully controlling the electrochemical reaction of Cu ions, besides transparent and mirror state, a blue state could also be achieved in the REM device. Electrolyte formulation is crucial for REM devices. Costly ionic liquid was normally used to achieve longer memory effect in the REM device[37]. In our work, we have carefully selected a polymer host for the electrolyte that leads to the formation of a smooth and uniform mirror state, and helps to sustain the mirror state of the REM device during the voltage-off state.

2. Experimental

2.1 Chemicals

Copper (II) chloride ($CuCl_2$, Sigma-Aldrich) was used as received. DMSO (Alfa Aesar) was used as solvent. Lithium perchlorate ($LiClO_4$, Sigma-Aldrich) was used as the supporting electrolyte. Potassium iodide (KI, Sigma-Aldrich) was used as the electrochemical mediator. Poly (vinyl alcohol) (PVA, molecular weight of 146,000-186,000, Sigma-Aldrich) was used as the polymer host for the electrolyte. ITOs (15 Ω/□) were used as the transparent conducting electrodes in the 3-electrode setup and device fabrication.

2.2 Preparation of electrochromic solution, polymer gel electrolyte and REM device

The electrochromic solution was prepared as follows: 0.8 mmol of $CuCl_2$ (107.56 mg) as the electrochromic material, 2.5 mmol of $LiClO_4$ (265.98 mg) as the supporting electrolyte, and 0.006 mmol of KI (1.0 mg) as electrochemical mediator was dissolved in 10.0 g of DMSO. Subsequently, 10 wt % of PVA (Mw= 146,000-186,000) was added as the polymer host and stirred at 80^{o}C till a homogeneous polymer gel electrolyte was obtained. The REM device was fabricated using Indium Tin Oxide (ITO) (15 Ω/□) as both working and counter electrodes. Ag wire was used as the reference electrode which was sandwiched in a serpentine manner between the spacers. The polymeric gel electrolyte was injected between the two ITO electrodes. The device has an active area of 4 × 1.5 cm^2 and sealed using a commercial sealant. Demonstration of large area REM devices with an active area of 4.5 × 4.5 cm^2 and 8 × 6 cm^2 was also carried out.

2.3 Characterizations

The *in situ* analyses were performed using UV-Vis-NIR Spectrometer (Cary 5000, Agilent Technologies) and potentiostat (Autolab PGSTAT 30, Metrohm Autolab) to obtain both the transmittance and reflectance spectra (diffuse reflectance accessory, DRA-2500 was used with poly (tetrafluoroethylene) (PTFE) as the baseline) as well as the kinetic spectra for the cycling test. X-ray diffraction (XRD,

View Article Online
DOI: 10.1039/C7TC01070B
Journal Name ARTICLE

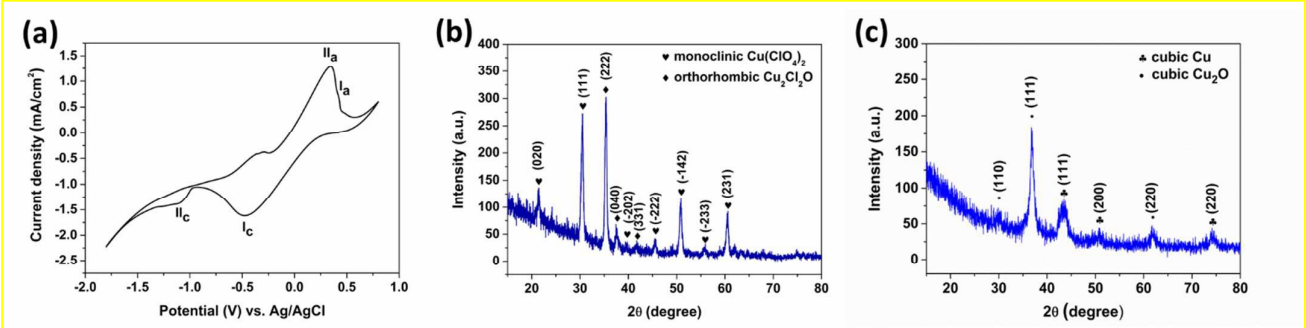

Fig. 1 (a) Cyclic voltammogram of Cu film on the ITO electrode in the electrochromic solution in the potential range of -1.8 to +0.6 V vs. Ag/AgCl, (b) XRD patterns of the electrodeposited Cu blue film and (c) Cu mirror film in the electrochromic solution.

Shimadzu discover diffractometer with CuKα-radiation (λ = 1.5406 Å) was used to identify the structure and composition of the electrodeposited Cu films. Field emission scanning electron microscopy (FESEM, Model Supra 55, Carl Zeiss) was used to identify the morphology of the electrodeposited Cu films. The surface roughness of the Cu films was analyzed by atomic force microscopy (Cypher S, Asylum Research).

3. Results and discussion

In order to evaluate the electrochemical performance of the electrochromic solution, the cyclic voltammetry (CV) measurements of Cu on the ITO electrode was conducted in the potential region of -1.80 to +0.60 V (vs. Ag/AgCl) at a scan rate of 20 mV/s in the three-electrode configuration with platinum electrode as the counter electrode. The typical redox peak for Cu was observed in the CV curve (Fig. 1(a)), which can be ascribed to the reduction and oxidation of Cu ions, leading to electrodeposition and dissolution of Cu on the ITO electrode. As the potential is swept from open circuit potential to the negative direction, the first cathodic peak, I_c is observed at -0.47 V. This cathodic peak is attributed to the reduction of Cu^{2+} ions to Cu^{+} ions. When the reduction potential reaches –1.10 V, a second cathodic peak, II_c is observed. The peak, II_c corresponds to the formation of metallic copper mirror when Cu^{+} ions are reduced to Cu^{0}. As the cathodic sweep continues, the mirror-like surface increases in reflectivity as more and more Cu are being electrodeposited onto the ITO electrode. When the potential sweeps from -1.80 V towards a positive/anodic direction, anodic peak, II_a appears at -0.30 V. This II_a peak corresponds to the oxidation of the Cu^{0} to Cu^{+} ions, leading to an increase in the transmittance of the ITO electrode as Cu film dissolves back into the solution. The second anodic peak, I_a, appears at +0.42 V and can be attributed to the oxidation of Cu^{+} to Cu^{2+} which signals the complete Cu film erasure from the ITO electrode back into the electrochromic solution. The electrochemical reaction of the electrodeposition of Cu ions in the electrochromic solution can be depicted as follows:

Blue film formation: $CuCl_2 + e^- \rightarrow CuCl + Cl^-$
Mirror film formation: $CuCl + e^- \rightarrow Cu + Cl^-$

Oxidation of CuCl film when exposed in ambient environment:
$4CuCl + O_2 \rightarrow 2Cu_2Cl_2O$
$4CuCl + O_2 + 8ClO_4^- + 2H_2O \rightarrow 4Cu(ClO_4)_2 + 4Cl^- + 4OH^-$

And,
$2CuCl_2 + 2KI \rightarrow 2CuCl + I_2 + 2KCl$
$2CuCl \rightarrow Cu + CuCl_2$

Regeneration of KI:
$Cu + 2KCl + I_2 \rightarrow CuCl_2 + 2KI$

The electrodeposition and dissolution mechanisms can be described based on the reduction and oxidation of Cu ions in the electrochromic solution. The blue film (CuCl) is formed when Cu^{2+} ions ($CuCl_2$) are electrochemically reduced to Cu^{+} ions. The unstable CuCl film undergoes oxidation in the ambient environment to form $Cu(ClO_4)_2$ and Cu_2Cl_2O, which were detected by XRD in practice rather than CuCl. The oxidized blue film has been identified to consist of a combination of monoclinic phase of $Cu(ClO_4)_2$ and orthorhombic phase of Cu_2Cl_2O in the XRD analysis (Fig. 1(b)). The CuCl undergoes reduction to form copper mirror state, Cu^{0} with the application of negative potential beyond -1.10 V. The XRD patterns of Cu mirror film electrodeposited at -1.8 V on the ITO electrode consisted of both cubic Cu and Cu_2O (cuprite) phases (Fig. 1(c)). However, it is noted that the reflective Cu mirror is not stable in the atmospheric air and prone to be oxidized to form Cu_2O after prolonged exposure in the ambient environment.

KI plays the role of reducing agent in the electrochemical reduction of Cu^{2+}. In our work, $CuCl_2$ acted both as the electrochromic material and oxidizing agent. Hence, KI mediated the reduction of Cu^{2+} ions to Cu^{+} ions, upon the application of negative potential. The unstable CuCl was further reduced to Cu^{0} which leads to the formation of the mirror state. KI was consumed during the reduction of Cu^{2+}, and can be regenerated when Cu^{0} reacts with KCl and I_2 during the dissolution step.

View Article Online
DOI: 10.1039/C7TC01070B

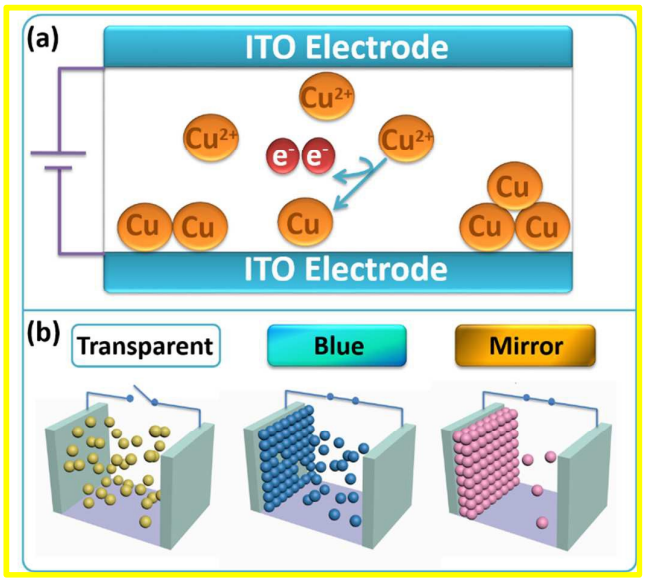

Fig. 2 (a) Schematic diagram of the electrodeposition of Cu ions to form a film in a Cu-REM device (b) Distribution of Cu ions in the transparent state (no potential), blue state (-0.9 V) and reflective state (-1.8 V) of the REM device (yellow balls refer to Cu^{2+} ions which are present at no potential, blue balls refer to the electrodeposition of Cu nanoparticles to form the blue CuCl (Cu^{+}) film whereas pink balls refer to the electrodeposition of the Cu^{0} mirror film).

Polymeric gel electrolytes are practical for electrochromic device assembly in view of several inevitable drawbacks of liquid electrolytes such as the possibility of electrolyte leakage, low chemical stability, and hydrostatic pressure considerations[7]. Therefore, the Cu-based REM device is designed to operate in the polymeric gel electrolyte. Fig. 2(a) is a schematic diagram of the electrodeposition of Cu ions to form the Cu film in a Cu-REM device. Before applied potential, all the Cu^{2+} ions are distributed homogeneously in the gel electrolyte. When a negative potential is applied on the working ITO, the applied potential causes the Cu^{2+} ions to be electrodeposited from the gel electrolyte onto the working electrode. It was found that a blue film (CuCl) is formed at a lower applied potential of -0.9 V (Fig. 2(b)). At -1.8 V, Cu^{2+} ions are reduced to Cu^{0} that leads to the formation of mirror state (Fig. 2(b)). When a positive potential is applied to the working electrode, the electrodeposited Cu metal dissolved into the gel electrolyte, thereby increasing the optical transmittance of the working electrode. At this transparent state, all Cu^{2+} ions are distributed randomly in the gel electrolyte and ideally the dissolution from the ITO electrode is reversible.

Nucleation and growth of Cu nuclei precede the film formation. For uniform film morphology, the nuclei must be distributed homogeneously throughout the substrate, followed by a controlled growth. Higher reflectivity can be obtained when Cu nuclei grew into nanosize grains that are

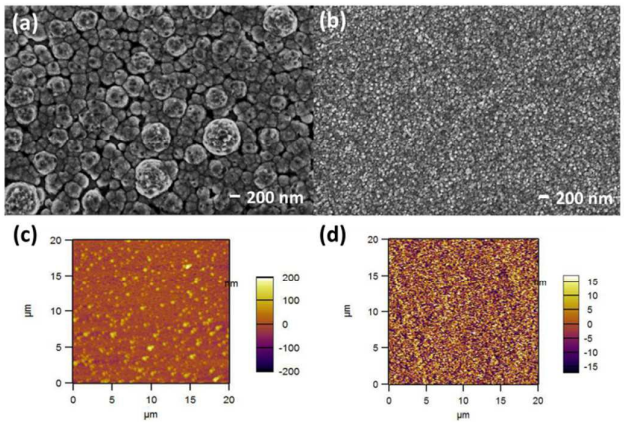

Fig. 3 High magnification FESEM images of the electrodeposited Cu film on the ITO electrode from (a) electrochromic solution and (b) polymeric gel electrolyte under the applied potential of -1.8 V for 120 s, AFM images of the electrodeposited Cu film on the ITO electrode from (c) electrochromic solution and (d) polymeric gel electrolyte under the applied potential of -1.8 V for 120 s.

compact and densely electrodeposited. Large aggregation of Cu particles would lead to agglomeration, resulting in diffusive reflectance. To understand Cu film formation on the ITO electrodes, the surface morphologies were examined using FESEM. The Cu films were electrodeposited from electrochromic solution and polymeric PVA gel electrolyte onto the ITO electrodes by applying a potential of -1.8 V (vs. Ag/AgCl) for 120 s. From Fig. 3(a), larger aggregation and agglomeration of Cu nanoparticles (200 – 750 nm) occurred when electrodeposition was carried out without the presence of PVA. AFM analysis shows that the Cu film has a root mean roughness (RMS) of 27.2 ± 1.1 nm based on three film samples. These Cu films have film thickness of 240.0 ± 15.4 nm (Fig. S1(a) in ESI). In the presence of PVA, Cu nanoparticles are compactly covering the electrode surface with no agglomeration after being electrodeposited for 120 s (Fig. 3(b). The size of the Cu nanoparticles ranges from 30 – 50 nm. The uniform and compact film morphology can be attributed by the slower rate of electrodeposition. The presence of PVA increases the viscosity of the electrolyte and increases solution resistance to the movement of ions, leading to decrease in ion mobility which slows down the rate of electrodeposition. Hence, the Cu films have thinner film thickness of 105.0 ± 6.5 nm (Fig. S1(b)). The low surface roughness of the Cu film when electrodeposited in the presence of PVA has been analyzed using AFM. Fig. 3(d) shows that the Cu film has a very low surface roughness with RMS of 9.3 ± 0.6 nm with better film uniformity. One of the notable advantages of the polymeric gel electrolyte is that the system does not require a nucleation layer which is often vital in initiating and facilitating uniform electrodeposition of metal nanoparticles onto the conducting substrate. Continuous electrical charge supply often yield cracks and wrinkles on the metal films due to the poor

View Article Online
DOI: 10.1039/C7TC01070B

adhesion and aggregation of metal nanoparticles onto transparent conducting electrode[37, 60]. However, the addition of PVA prevents agglomeration of Cu nanoparticles as it promotes slower and controlled rate of electrodeposition, which resulted in uniform film morphology.

The optical transmittance spectra of Cu-based REM device were measured under an applied potential of -0.9 V, -1.2 V and +0.1 V for 60 s, respectively, as shown in Fig. 4(a). The device shows a high transmittance of 81.86 % at its neutral state when measured at the wavelength of 550 nm, using air as the baseline. The intermediate state, a blue color film was formed at a potential of -0.9 V and exhibited a low transmittance of 24.64 %. This tinted state can be useful for the smart windows application, by providing indoor comfort while conserving the energy consumption of the buildings as only very low electrical potential is required to execute the tinted state. The mirror film was formed at a potential of -1.2 V and exhibited an extremely low transmittance of 0.33 %. The Cu-based REM device presented a high transmittance modulation of 81.53 % at 550 nm under the applied potential of -1.2 and +0.1 V. From the reflectance spectra, the mirror effect initiates at -1.2 V with a low reflectance modulation of 2.35 % at 550 nm as shown in the Fig. 4(b). Upon higher applied potential of -1.8 V, the device exhibited a reflectance contrast of 29.41 % at 550 nm. At the same applied potential, the reflectance contrast was more pronounced, that is 54.80 % at the wavelength of 660 nm. It is evident from the reflectance spectra that the device reflectivity increases with higher applied potential. On the contrary, reflectance modulation was not achieved when de Mello and co-workers reported on the aqueous Cu-based reversible metal electrodeposition[61]. This is because choice of solvents plays a substantial role in the formulation of electrolytes in the REM system. The electrochemical potential window of water is limited by hydrogen and oxygen evolution in the cathodic and anodic regions, extending beyond the limit will result in electrolysis. Compared to aqueous electrolytes, organic solvents (*N,N*-dimethylformamide (DMF), DMSO and ionic liquids offer wider electrochemical potential window during cathodic electrodeposition as they do not undergo decomposition easily. For instance, Li *et. al.* reported a cathodic limiting potential and anodic limiting potential of -3.40 and +1.20 V respectively, with an electrochemical window of 4.60 V in the DMSO-LiCl based electrolyte[62].

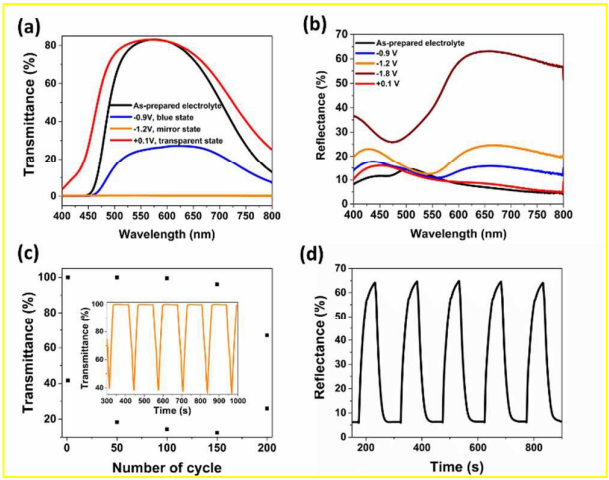

Fig. 4 (a) Transmittance spectra of Cu electrodeposited on the ITO electrode in the colored (-0.9, -1.2 V) and bleached (+0.1 V) states in the wavelength of 400 – 800 nm, (b) Reflectance spectra of Cu electrodeposited on the ITO electrode in the colored (-0.9 V), mirror (-1.2, -1.5 and -1.8 V) and bleached (+0.1 V) states in the wavelength of 400 – 800 nm, (c) Cycling performance of Cu-based REM device for 200 cycles using potential algorithms of -1.2 V (20 s), -1.5 V (10s), -0.1 V (60 s), 0.2 V (20 s) and 0 V (20 s) at 550 nm (Inset: *In situ* transmittance of electrodeposition and dissolution of Cu film on the ITO electrode), (d) *In situ* reflectance of Cu-based REM device when switched using potential algorithms of -1.5 V (30 s), -1.8 V (30 s), 0 V (60 s), and +0.1 V (30s).

Switching time is one of the most important parameters for electrochromic applications that define the kinetics of the electrochemical process during the transition from one state to another under alternating potentials. Switching time is defined as the time taken for the electrochromic system to reach 90 % of its full modulation between the steady colored and bleached states. The coloration and bleaching speed of the Cu film in the polymeric gel electrolyte were investigated by *in situ* transmittance at 550 nm by using sequential application of the following potential algorithms: -1.2 V (20 s), -1.5 V (10 s), -0.1 V (60 s), 0.2 V (20 s) and 0 V (20 s). From inset of Fig. 4(c), the switching time for the coloration and bleaching is 24.2 and 17.4 s respectively. The switching speed is fairly moderate even with the incorporation of 10 wt% of PVA in the electrolyte. This viscous electrolyte slows the electrodeposition of the Cu nanoparticles onto the ITO electrode as well as the dissolution of Cu film back to the electrolyte compared to the electrochromic solution. The more electroactive copper promotes reversibility of the electrodeposition and dissolution processes, making it unique in the ease of film formation and erasure in the REM device[31,36]. The cycling stability of the REM device is demonstrated in Fig. 4(c). The device shows initial transmittance modulation of 58.34 % and attains a maximum transmittance modulation of 83.61 % at 53th cycle. The transmittance modulation of the device gradually decreases and manages to sustain a modulation of 40.90 % after 200 cycles. The reversibility of the system can be confirmed through the reversible electrodeposition and dissolution of the Cu nanoparticles onto the ITO electrode, which was monitored through *in situ* uv-vis spectrophotometry analysis. From the kinetic spectra in Fig. 4(c)), low transmittance indicated the formation of Cu mirror and high transmittance indicated the dissolution of Cu mirror film from the ITO electrode. The kinetic spectra show continuous reversible switching between high transmittance and low transmittance, which verified the reversibility of electrodeposition and dissolution of Cu

View Article Online
DOI: 10.1039/C7TC01070B

nanoparticles. Long cycling test was conducted up to 900 cycles of continuous reversible electrodeposition and dissolution on a single ITO electrode in the three-electrode electrochemical analysis as shown in Fig. S2. Fig. 4(d) shows that the Cu mirror film has a reflectance modulation of 58.90 % at the wavelength of 660 nm via the potential algorithms of -1.5 V (30 s), -1.8 V (30 s), 0 V (60 s), and +0.1 V (30 s). The time taken for mirror formation and dissolution is 23.3 and 13.7 s, respectively. The switching times of the current state of the art of the REM is not known, as latest literatures do not reveal the switching performance of the REM system in the reflectance mode[36-38]. This is most likely due to the slow switching of the REM. Switching time is one of the most critical attributes which determine the competitive features of the smart windows and electronic displays.

The switching time could be influenced by several factors such as applied potential, film thickness, ionic conductivity of electrolyte and charge transfer resistivity[49]. Additionally, switching time depends on the rate of electrodeposition of metal nanoparticles and the rate of the film dissolution for the REM device. Ideally, higher ionic conductivity promotes faster rate of electrodeposition and dissolution as ions diffusion could occur readily. To study the ionic conductivity of the polymeric gel electrolyte, electrochemical impedance spectroscopy (EIS) was conducted in the frequency range of 100 kHz to 0.1 Hz at the open-circuit potential. Fig. 5(a) shows the Nyquist plot of the Cu-REM device with the semicircle in the high-frequency region. The semi-circle is ascribed to the charge transfer impedance. From the EIS spectrum, the polymeric gel electrolyte has an ionic conductivity of 5.60 x 10^{-5} S cm^{-1}. The conductivity of an electrolyte is a function of the degree of dissociation, mobility of the individual ions, viscosity, temperature and the electrolyte composition[63]. To understand the effect of ionic conductivity, kinetic test was performed on both electrochromic solution and polymeric gel electrolyte using the same applied potentials (± 1.8 V for 20 s per step) and transmittance modulation (72 ±1.0 %). The electrochromic solution has ionic conductivity of 1.96 x 10^{-4} S cm^{-1} with coloration time of 14.2 s and bleaching time of 4.4 s as shown in the Fig. S3 and S4. The polymeric gel electrolyte exhibited coloration time of 29.4 s and bleaching time of 4.8 s (Fig. S5). From the ionic conductivity and switching time results, higher ionic conductivity promotes ion mobility, which inherently improves the rate of electrodeposition of the Cu nanoparticles.

Another noteworthy property of the Cu-based REM device is the ability to demonstrate appreciable transmittance modulation at low potential. This feature is a valuable property for low energy fenestration application. The device exhibited a transmittance modulation of 55.95 % under applied potential of -0.8 V for 60 s which can last for 4.11 minutes (Fig. 5(b)) at the wavelength of 550 nm. Increasing the negative potential to -1.8 V for 60 s has a remarkable contrast difference of 92.20 %, with the mirror effect lasting for 21.17 minutes. Therefore, the Cu-based REM device demonstrated the capability of memory

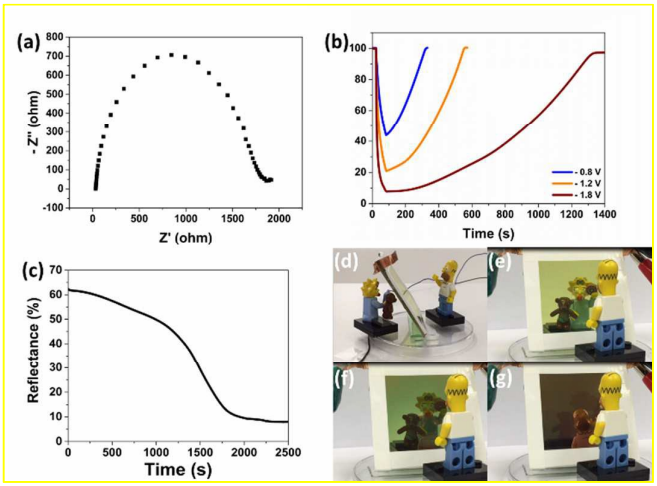

Fig. 5 (a) Nyquist plot of the polymeric gel electrolyte in the high frequency region, (b) Demonstration of appreciable transmittance modulation at low potential of -0.8, -1.2 and -1.8 V and their memory effect retentions, and (c) Memory effect retention of Cu-REM device in the reflectance mode during the voltage off-state after applied potential of -1.8 V for 10 minutes, (d) Setup of the demonstration of the large area Cu-based REM device, (e) Transparent state of the large area, 4.5 cm-by-4.5 cm Cu-REM device prior to application of potential, (f) Blue state, and (g) Mirror state.

effect retention without the use of ionic liquid. In the reflectance mode, Cu-based REM device exhibited an appreciable memory effect of 40 minutes (at 660 nm) upon the application of -1.8 V for 10 minutes (Fig. 5(c)). Park *et. al.* reported on the long memory effect of 2 hours in the switchable silver mirror upon application of -2.5 V for 30 minutes when ionic liquids were introduced in the electrolyte[37]. The memory effect of our current work is attributed to the viscous PVA gel electrolyte (3.97 kcP) that acts as an effective barrier to slow the anions from diffusing into the Cu film and protected the Cu film from dissolving back into the electrolyte during the voltage-off state, leading to longer memory retention. This zero-current consumption after coloration, the "memory effect" of electrochromism, is often cited as a valuable, desirable property of (large) electrochromic systems which helps in the energy fenestration[64].

Device scalability was demonstrated by fabricating a large area device encompassing an active area of 4.5 × 4.5 cm and 8 × 6 cm. Fig. 5(d) shows the setup of the large area device for demonstration purpose where Homer Simpson was placed in front of the device (3 cm apart) to demonstrate the mirror effect when a negative potential was applied while Maggie Simpson was placed at the back of the device (1 cm apart) to demonstrate the privacy glass effect. Fig. 5(e) shows the transparent state of the device prior to application of

View Article Online
DOI: 10.1039/C7TC01070B

potential. Upon the application of negative potential of -1.8 V for 7 s, the device displayed blue state (Fig. 5(f)). With longer deposition time, the Cu nanoparticles formed mirror film (Fig. 5(g)). The mirror reflectivity increased with longer deposition time. Upon the application of positive potential of +0.1 V, film erasure took place when the Cu mirror film dissolved back into the electrolyte. Video demonstrations were recorded and are available for viewing (ESI Movies 1 and 2) for both 4.5 × 4.5 cm and 8 × 6 cm devices).

Conclusions

Cu-REM device offers the advantage of both transmittance and reflectance modulations. The ability to deliver three modulation states of transparent, blue and mirror is deemed impactful for the emerging optoelectronic devices. The maximum potential needed to operate the device is -1.8 V which is operational using normal battery; this plays a very important role in the energy-fenestration technologies such as building façades and electronic display applications. The low potential required for the operation of the REM device shows a highly desirable property for any portable application where battery life is paramount. The facile device fabrication offers a significant advantage in the scalability of the large area ECD as it does not require complicated and expensive vacuum technology. The Cu-REM device delivers promising features for various emerging optoelectronic devices as it offers dual transmission and reflectance modulations, ability to demonstrate appreciable transmittance modulation at low potential, and memory effect retention.

Acknowledgements

This research is supported by the National Research Foundation, Prime Minister's Office, Singapore under its Campus for Research Excellence and Technological Enterprise (CREATE) programme.

Notes and references

1. V. K. Thakur, G. Ding, J. Ma, P. S. Lee and X. Lu, *Adv. Mater*, 2012, **24**, 4071-4096.
2. C. G. Granqvist, *Sol. Energy Mater. and Sol. Cells*, 2000, **60**, 201-262.
3. C. G. Granqvist, E. Avendaño and A. Azens, *Thin Solid Films*, 2003, **442**, 201-211.
4. G. F. Cai, M. Q. Cui, V. Kumar, P. Darmawan, J. X. Wang, X. Wang, A. L.-S. Eh, K. Qian and P. S. Lee, *Chem. Sci.*, 2016, **7**, 1373-1382.
5. G. F. Cai, J. X. Wang and P. S. Lee, *Acc. Chem. Res.*, 2016, **49**, 1469-1476.
6. G. F. Cai, P. Darmawan, M. Q. Cui, J. W. Chen, X. Wang, A. L.-S. Eh, S. Magdassi and P. S. Lee, *Nanoscale*, 2016, **8**, 348-357.
7. A. L.-S. Eh, X. Lu and P. S. Lee, in *Electrochromic Materials and Devices*, eds. R. J. Mortimer, D. R. Rosseinsky and P. M. S. Monk, Wiley-VCH Verlag GmbH & Co. KGaA, Weinheim, Germany, 2013, ch. 10, pp. 289-310.
8. N. L. Sbar, L. Podbelski, H. M. Yang and B. Pease, *Int. J. Sustainable Built Environ.*, 2012, **1**, 125-139.
9. A. Llordes, G. Garcia, J. Gazquez and D. J. Milliron, *Nature*, 2013, **500**, 323-326.
10. C. M. Lampert, *Sol. Energy Mater. and Sol. Cells*, 1998, **52**, 207-221.
11. R. Baetens, B. P. Jelle and A. Gustavsen, *Sol. Energy Mater. and Sol. Cells*, 2010, **94**, 87-105.
12. Y. Tian, W. Zhang, S. Cong, Y. Zheng, F. Geng and Z. Zhao, *Adv. Funct. Mater.*, 2015, **25**, 5833-5839.
13. C. M. Lampert, *Sol. Energy Mater. and Sol. Cells*, 2003, **76**, 489-499.
14. M. Gratzel, *Nature*, 2001, **409**, 575-576.
15. L. Yang, D. Ge, J. Zhao, Y. Ding, X. Kong and Y. Li, *Sol. Energy Mater. and Sol. Cells*, 2012, **100**, 251-257.
16. H. Demiryont and D. Moorehead, *Sol. Energy Mater. and Sol. Cells*, 2009, **93**, 2075-2078.
17. W. B. Kang, C. Y. Yan, X. Wang, C. Y. Foo, A. W. M. Tan, K. J. Chee and P. S. Lee, *J. Mater. Chem. C*, 2014, **2**, 4727.
18. H. Li, J. Chen, M. Cui, G. Cai, A. L.-S. Eh, P. S. Lee, H. Wang, Q. Zhang and Y. Li, *J. Mater. Chem. C*, 2016, **4**, 33-38.
19. R. J. Mortimer, *Annu. Rev. Mater. Res.*, 2011, **41**, 241-268.
20. G. F. Cai, C. D. Gu, J. Zhang, P. C. Liu, X. L. Wang, Y. H. You and J. P. Tu, *Electrochim. Acta*, 2013, **87**, 341-347.
21. D. S. Dalavi, R. S. Devan, R. S. Patil, Y.-R. Ma and P. S. Patil, *Mater. Lett.*, 2013, **90**, 60-63.
22. K. Tajima, H. Hotta, Y. Yamada, M. Okada and K. Yoshimura, *Sol. Energy Mater. and Sol. Cells*, 2011, **95**, 3370-3376.
23. K. Tajima, Y. Yamada and K. Yoshimura, *Sol. Energy Mater. and Sol. Cells*, 2014, **126**, 227-236.
24. P. H. L. Molten, M. Kremers and R. Griessen, *J. Electrochem. Soc.*, 1996, **143**, 3348-3353.
25. T. J. Richardson, J. L. Slack, B. Farangis and M. D. Rubin, *Appl. Phys. Lett.*, 2002, **80**, 1349-1351.
26. T. Kazuki, Y. Yasusei, O. Masahisa and Y. Kazuki, *Appl. Phys. Express*, 2010, **3**, 042201.
27. T. J. Richardson, *Solid State Ionics*, 2003, **165**, 305-308.
28. S. I. C. deTorresi and I. A. Carlos, *J. Electroanal. Chem.*, 1996, **414**, 11-16.
29. J. P. Ziegler and B. M. Howard, *Sol. Energy Mater. and Sol. Cells*, 1995, **39**, 317-331.
30. B. M. Howard and J. P. Ziegler, *Sol. Energy Mater. and Sol. Cells*, 1995, **39**, 309-316.
31. J. P. Ziegler, *Sol. Energy Mater. and Sol. Cells*, 1999, **56**, 477-493.
32. R. M. Elofson and R. L. Edsberg, *Can. J. Chem.*, 1957, **35**, 646-650.
33. G. G. Barna and J. G. Fish, *J. Electrochem. Soc.*, 1981, **128**, 1290-1292.
34. P. M. S. Monk, C. Turner and S. P. Akhtar, *Electrochim. Acta*, 1999, **44**, 4817-4826.
35. P. M. S. Monk, F. Delage and S. M. Costa Vieira, *Electrochim. Acta*, 2001, **46**, 2195-2202.
36. S. Araki, K. Nakamura, K. Kobayashi, A. Tsuboi and N. Kobayashi, *Adv. Mater.*, 2012, **24**, OP122-126, OP121.
37. C. Park, S. Seo, H. Shin, B. D. Sarwade, J. Na and E. Kim, *Chem. Sci.*, 2015, **6**, 596-602.
38. T.-Y. Kim, S. M. Cho, C. S. Ah, K.-S. Suh, H. Ryu and H. Y. Chu, *J. Inf. Disp.*, 2014, **15**, 13-17.
39. A. Tsuboi, K. Nakamura and N. Kobayashi, *Adv. Mater.*, 2013, **25**, 3197-3201.
40. A. Tsuboi, K. Nakamura and N. Kobayashi, *J. Soc. Inf. Disp.*, 2013, **21**, 361-367.

View Article Online
DOI: 10.1039/C7TC01070B

41. A. Tsuboi, K. Nakamura and N. Kobayashi, *Chem.f Mater.*, 2014, **26**, 6477-6485.
42. R. Onodera, A. Tsuboi, K. Nakamura and N. Kobayashi, *J. Soc. Inf. Disp.*, 2016, **24**, 424-432.
43. O. Ryou, S. Yoshiyuki, S. Shigeyuki, Y. Katsumi, S. Yutaka and U. Takayuki, *Appl. Phys. Express*, 2013, **6**, 026503.
44. Z. He, X. Yuan, Q. Wang, L. Yu, C. Zou, C. Li, Y. Zhao, B. He, L. Zhang, H. Zhang and H. Yang, *Adv. Opt. Mater.*, 2016, **4**, 106-111.
45. R.-T. Wen, C. G. Granqvist and G. A. Niklasson, *Nat Mater*, 2015, **14**, 996-1001.
46. J. N. Huiberts, R. Griessen, J. H. Rector, R. J. Wijngaarden, J. P. Dekker, D. G. de Groot and N. J. Koeman, *Nature*, 1996, **380**, 231-234.
47. P. S. Lee, G. F. Cai, A. L.-S. Eh and P. Darmawan, in *Nanomaterials for 2D and 3D Printing*, eds. S. Magdassi and A. Kamyshny, Wiley-VCH Verlag GmbH & Co. KGaA, Weinheim, Germany, 2017, ch. 16, pp. 317-339.
48. J. Denayer, P. Aubry, G. Bister, G. Spronck, P. Colson, B. Vertruyen, V. Lardot, F. Cambier, C. Henrist and R. Cloots, *Sol. Energy Mater. and Sol. Cells*, 2014, **130**, 623-628.
49. M. Q. Cui, W. S. Ng, X. Wang, P. Darmawan and P. S. Lee, *Adv. Funct. Mater.*, 2015, **25**, 401-408.
50. R. A. M. Hikmet and H. Kemperman, *Nature*, 1998, **392**, 476-479.
51. T. Ye, Y. Xiang, H. Ji, C. Hu and G. Wu, *RSC Adv.*, 2016, **6**, 30769-30775.
52. G. F. Cai, P. Darmawan, M. Q. Cui, J. X. Wang, J. W. Chen, S. Magdassi and P. S. Lee, *Adv. Energy Mater.* 2016, **6**.
53. G. Y. Karaca, E. Eren, C. Alver, U. Koc, E. Uygun, L. Oksuz and A. U. Oksuz, *Electroanal.*, 2017, DOI: 10.1002/elan.201600631.
54. C. G. Granqvist, *Thin Solid Films*, 2014, **564**, 1-38.
55. US Pat., 0061919 A1, 2004.
56. US Pat., 7,046,418 B2, 2006.
57. D. R. MacFarlane, N. Tachikawa, M. Forsyth, J. M. Pringle, P. C. Howlett, G. D. Elliott, J. H. Davis, M. Watanabe, P. Simon and C. A. Angell, *Energy & Environ. Sci.*, 2014, **7**, 232-250.
58. T. Tsuda and C. L. Hussey, *Electrochem. Soc. Interface*, Spring 2007, **16**.
59. US Pat., 6,552,843 B1, 2002.
60. T.-Y. Wu, W.-B. Li, C.-W. Kuo, C.-F. Chou, J.-W. Liao, H.-R. Chen and C.-G. Tseng, *Int. J. Electrochem. Sci.*, 2013, **8**, 10720-10732.
61. D. A. A. de Mello, M. R. S. Oliveira, L. C. S. de Oliveira and S. C. de Oliveira, *Sol. Energy Mater. and Sol. Cells*, 2012, **103**, 17-24.
62. G. R. Li, G. K. Liu and Y. X. Tong, *Electrochem. Commun.*, 2004, **6**, 441-446.
63. H. L. Helen and H. Yinlun, in *Encyclopedia of Chemical Processing*, ed. S. Lee, Taylor & Francis, New York, 2006, vol. 2, pp. 839-848.
64. D. R. Rosseinsky and R. J. Mortimer, *Adv. Mater.*, 2001, **13**, 783-793.

View Article Online
DOI: 10.1039/C7TC01070B

The table of contents entry:

Copper-based reversible electrochemical mirror device offers the advantage of both transmittance and reflectance modulations, stimulating great interest in energy-fenestration technologies.

TOC figure